

1
2
3
4

Supplementary Materials for

A minimal pathway for the regeneration of redox cofactors

5 Michele Partipilo,¹ Eleanor J. Ewins,¹ Jacopo Frallicciardi,¹ Tom Robinson,² Bert Poolman¹ & Dirk Jan Slotboom^{1*}

6
7 ¹ Department of Biochemistry, Groningen Institute of Biomolecular Sciences & Biotechnology, University of
8 Groningen, Nijenborgh 4, 9747 AG Groningen, The Netherlands.

9 ² Department of Theory & Bio-Systems, Max Planck Institute of Colloids and Interfaces, Am Mühlenberg 1, 14476
10 Potsdam, Germany

11
12 *Corresponding author: d.j.slotboom@rug.nl

13
14
15
16
17
18 **This file includes:**

19
20 Supplementary Methods
21 Figs. S1 to S12
22 Tables S1 to S2
23 Plasmid maps S1 to S2
24
25
26
27

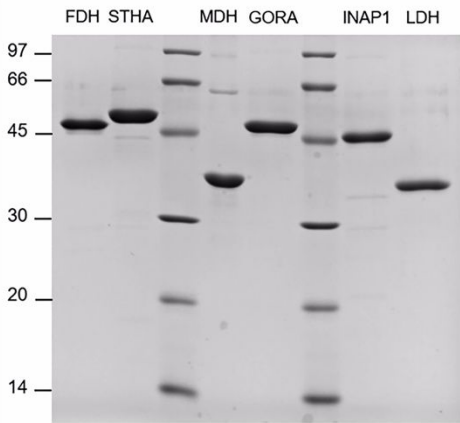
1 **Supplementary Methods**

2 SthA absorbance spectrum over storage

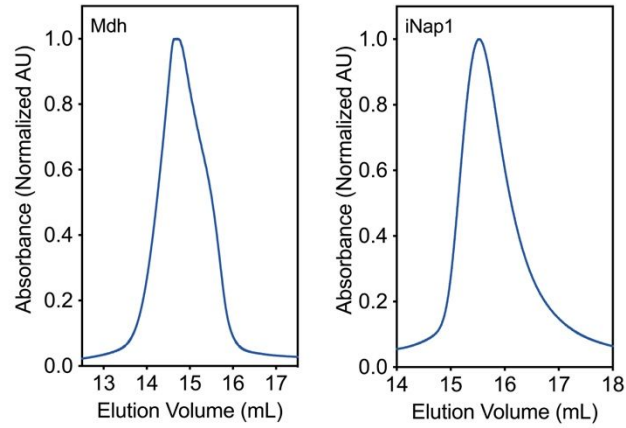
3 Several aliquots of 3.8 μ M purified soluble transhydrogenase SthA were thawed from the -80 $^{\circ}$ C
4 freezer and transferred to 4 $^{\circ}$ C in the dark. At different time points over a period of 70 days, 80 μ L
5 SthA were diluted in 50 mM KPi pH 7.5 (buffer B) for a final volume of 1000 μ L and loaded into
6 a quartz cuvette (Hellma Analytics, 109.004-QS) with the path length of 1 cm. By using a Cary 100
7 Bio UV-visible spectrophotometer (Varian, Inc., USA), absorbance spectra from 200 to 700 nm
8 were recorded at 25 $^{\circ}$ C.

9
10

A



B



1

2

3

4

5

6

7

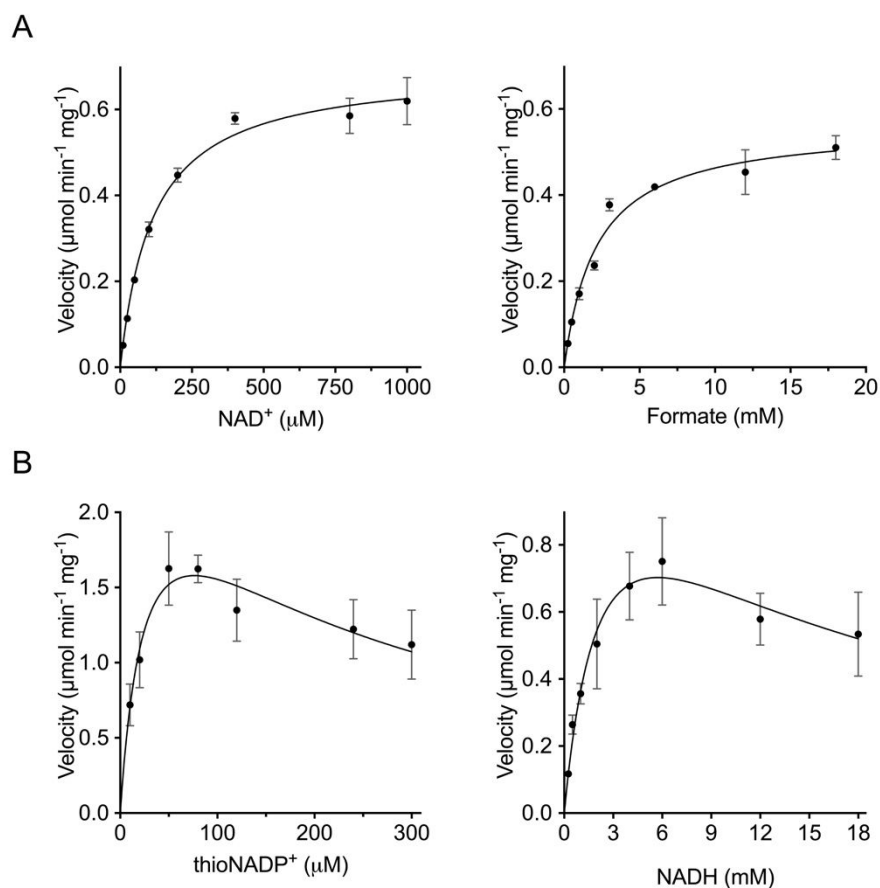
8

9

Fig. S1. Purity of the protein components employed in our cell-free system. (A) Coomassie-stained SDS-polyacrylamide gel (15% separating gel, 5% stacking gel) loaded with 0.3-0.6 $\mu\text{g}/\text{mL}$ of protein, depending on the specific sample. The proteins were overproduced through heterologous gene expression and purified from *E. coli* as described in the “Materials & methods” section. On the left, the molecular weight in kDa of the protein ladder. (B) Size-exclusion chromatography profiles of Malate dehydrogenase (Mdh) and iNap1. After the affinity chromatography, enabling the isolation of the proteins from the rest of the cytosolic fraction, both the samples were loaded on a SEC column Superdex 200 with the bed resin of 10 x 300 mm. The absorbance of the sample through the column was monitored at the wavelength of 280 nm.

10

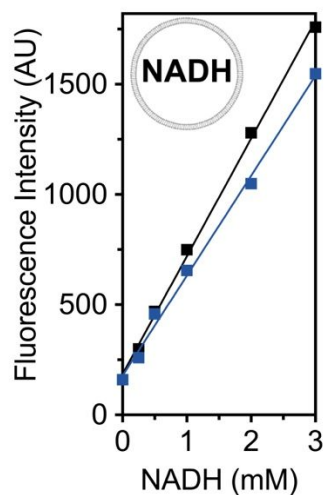
11



1

2 **Fig. S2. Kinetic data for purified Fdh and SthA.** (A) Michaelis-Menten plot of the reaction catalyzed by Fdh versus
 3 NAD^+ (left) and formate (right) concentrations. Fixing the formate concentration at 20 mM, we obtained a K_M for
 4 NAD^+ of $114.9 \pm 11.2 \mu\text{M}$, a V_{MAX} of $0.70 \pm 0.02 \mu\text{mol min}^{-1} \text{mg}^{-1}$ and a K_{CAT} of $1.08 \pm 0.03 \text{ s}^{-1}$. Testing different formate
 5 concentrations and keeping constant the amount of cofactor at 2.0 mM, we calculated a K_M for formate of 2.15 ± 0.36
 6 mM, a V_{MAX} of $0.56 \pm 0.03 \mu\text{mol min}^{-1} \text{mg}^{-1}$, and a K_{CAT} of $0.87 \pm 0.04 \text{ s}^{-1}$. (B) SthA displayed inhibition at high
 7 substrate concentrations for both thioNADP $^+$ (left) and NADH (right). For this reason, we fit the reaction rate using the
 8 substrate inhibition equation to estimate the kinetic parameters of the transhydrogenase. Employing the fixed
 9 concentration of 15 mM NADH, we calculated the K_M for thioNADP $^+$ at $28.9 \pm 10.8 \mu\text{M}$ its K_I at $201.0 \pm 80.2 \mu\text{M}$, the
 10 V_{MAX} at $2.77 \pm 0.54 \mu\text{mol min}^{-1} \text{mg}^{-1}$, and a K_{CAT} of $19.97 \pm 3.88 \text{ s}^{-1}$. By maintaining the amount of thioNADP $^+$ at 150
 11 μM , we quantified for NADH a K_M of $2.63 \pm 0.87 \text{ mM}$, a K_I of $12.45 \pm 4.89 \text{ mM}$, a V_{MAX} of $1.35 \pm 0.27 \mu\text{mol min}^{-1}$
 12 mg^{-1} , and a K_{CAT} of $9.70 \pm 1.91 \text{ s}^{-1}$. In all the graphs, error bars correspond to the standard deviation. The kinetics data
 13 were obtained from 4 independent replicates ($n = 4$), the error bars represent the standard deviation.

14



1

2

3

4

5

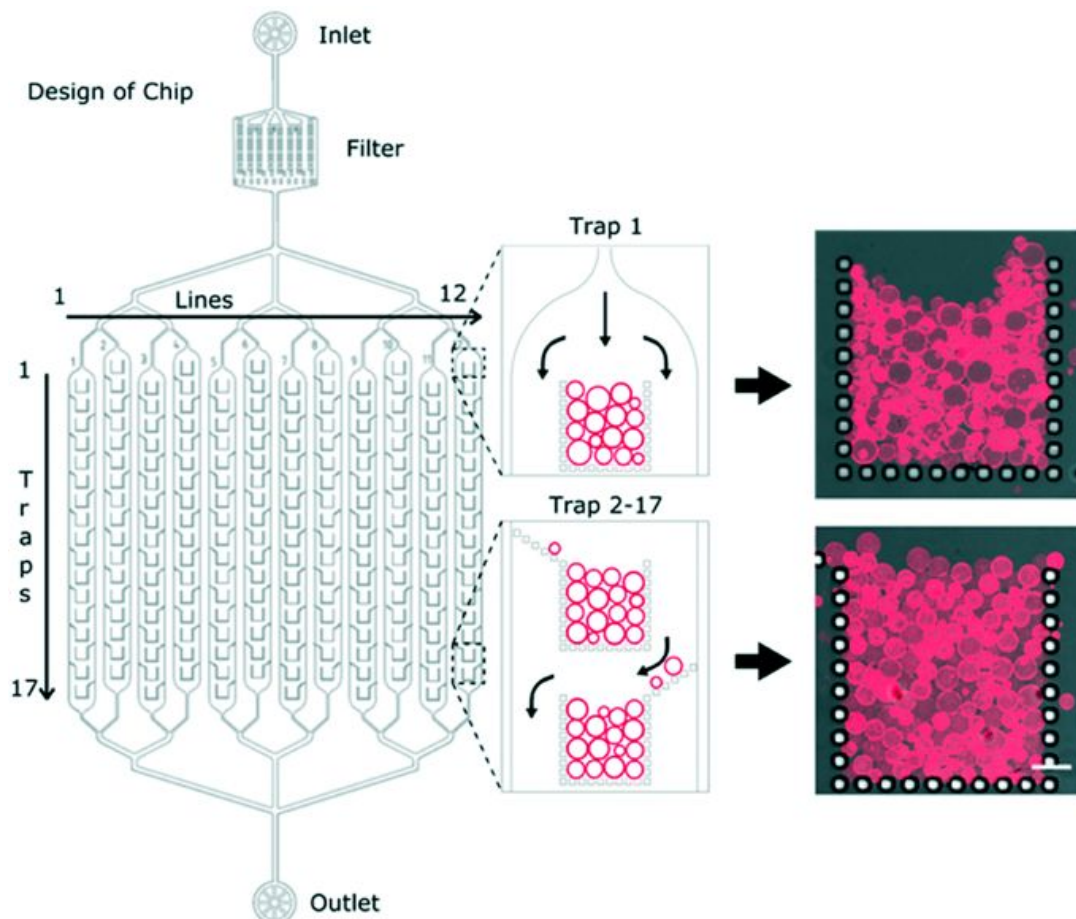
6

7

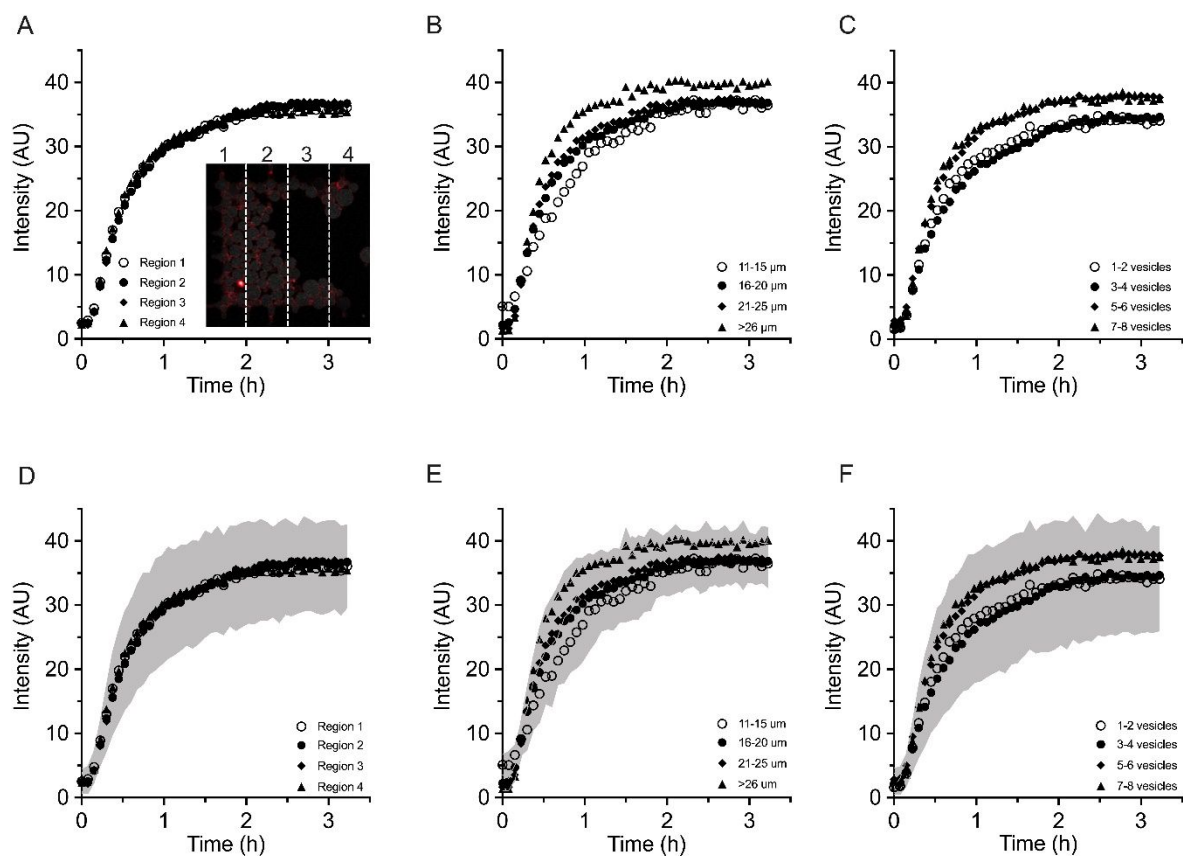
8

9

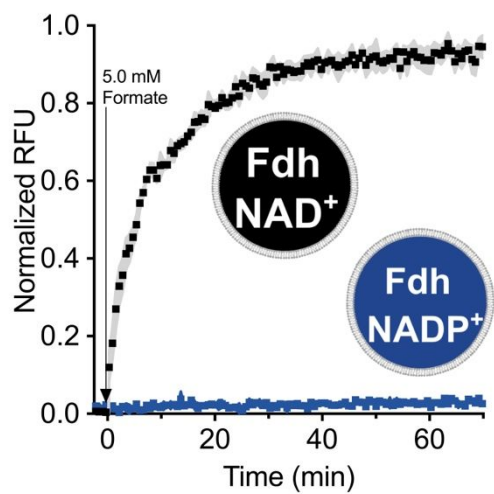
Fig. S3. Linear correlation between encapsulated NADH and fluorescence of LUVs. 400 nm extruded large unilamellar vesicles were prepared, entrapping different concentrations of NADH (0, 0.25, 0.5, 1.0, 2.0 and 3.0 mM) within their lumen. In this range, we found a linear correlation between the fluorescence intensity ($\lambda_{\text{EXC}} = 370$ nm; $\lambda_{\text{EMI}} = 530$ nm) and the amount of NADH. Such linearity is conserved regardless of the presence of the external scavenger system, although in the latter case (blue line, with scavenger) the fluorescence intensity was lower than without the scavenger (black line). The error bars are not shown for clarity ($n = 2$).



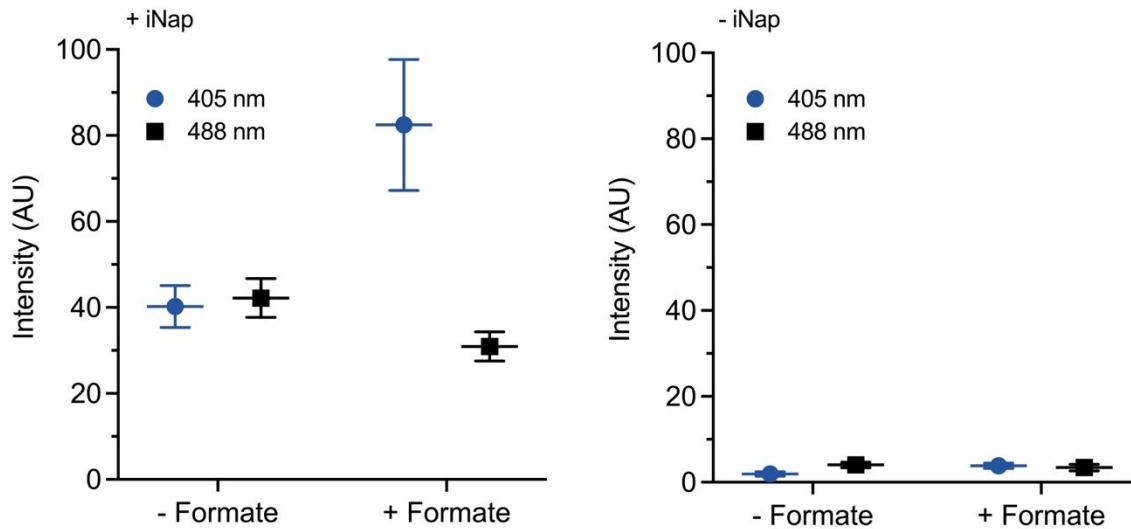
1
 2 **Fig. S4. Design of microfluidic chips used for monitoring changes in GUV fluorescence over time.** The bucket-
 3 like design of the PDMS posts allows populations of vesicles with a diameter $>10\ \mu\text{m}$ to be trapped in a fixed region
 4 in space, while the external solutions can be exchanged. Additionally, the alternating left and right “arm”-like features
 5 ensures vesicles to be directed into subsequent buckets for efficient filling.
 6 Fig.1 from DOI: [10.1039/c8lc01275](https://doi.org/10.1039/c8lc01275) is reproduced with permission from © Royal Society of Chemistry 2021 via the
 7 [Copyright Clearance Center](https://www.rsc.org/permissions).
 8
 9



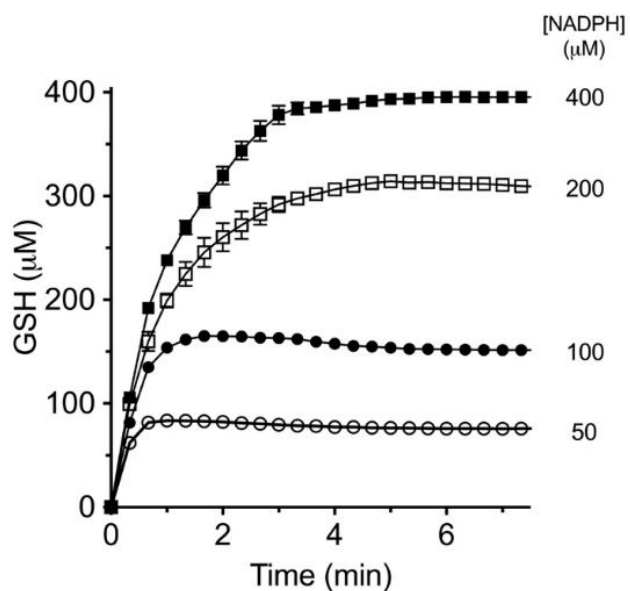
1
2 **Fig. S5. Influence of different experimental parameters and environments on NADH formation in GUVs. (A)**
3 The effect of vesicles' positions throughout the individual buckets on NADH formation is displayed. There is no
4 difference between vesicles being situated in different regions in the bucket. **(B)** The role of different vesicle sizes on
5 the rate of NADH formation and the final concentration is displayed. We can see from the graph that smaller vesicles
6 have a slightly slower initial rate of NADH formation, while larger vesicles result in higher final intensity values. **(C)**
7 The effect of local vesicle density on the increase in fluorescence from NADH. Vesicles that have a higher number of
8 neighbouring/adjacent GUVs (black triangles) result in a higher final intensity value. **(D-F)** Graphs in **(A-C)** with error
9 bars. Considering the large error bands for all sub-populations, at this stage we cannot say if these observations are
10 significant or not.
11



1
 2 **Fig. S6. Fdh cofactor specificity within 400-nm large unilamellar vesicles.** The encapsulation of 2.0 μM Fdh with
 3 1.0 mM cofactor (NAD⁺ in black, NADP⁺ in blue) highlights the strict NAD⁺-dependency of formate dehydrogenase
 4 upon the external addition of 5.0 mM ammonium formate. NADPH cannot be formed by Fdh-containing vesicles unless
 5 another specific NADP-dependent enzyme is entrapped in the vesicles.
 6



1
2 **Fig. S7. Luminal intensity of GUVs with (left panel) and without the iNap1 sensor (right panel) encapsulated**
3 **along with NAD⁺, NADP⁺, Fdh plus SthA.** Before adding formate to the sample containing iNap1, the intensity of
4 the 405 nm and 488 nm channels was recorded. After adding 5 mM formate, the intensity for 405 nm increases and for
5 488 nm decreases. In the right graph, no iNap1 is encapsulated and the resultant fluorescent values for the 405 nm and
6 488 nm channels both start at a much lower value without formate and do not significantly change when formate is
7 added.
8

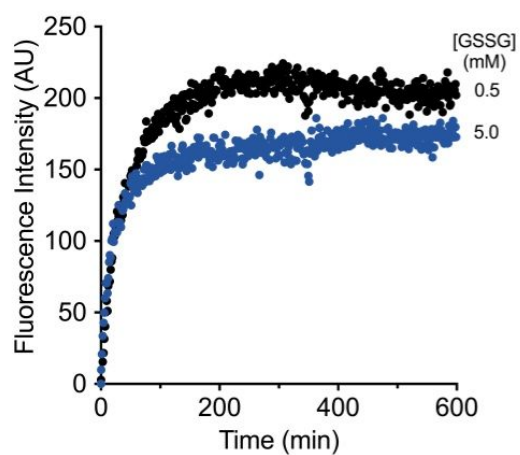


1

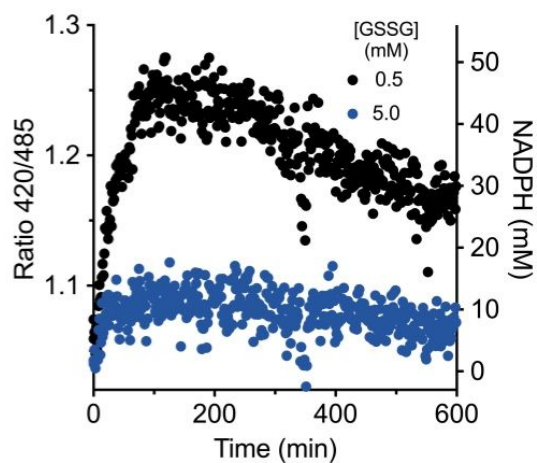
2 **Fig. S8. Glutathione reduction in bulk solution by GorA dependent on the NADPH concentration.** Through
 3 Ellman's assay, we followed the conversion of 200 μM GSSG into reduced glutathione mediated by 0.05 μM GorA
 4 upon the addition of different NADPH amounts (50 μM empty circles, 100 μM full circles, 200 μM empty squares,
 5 400 μM full squares) in KPi 50 mM, pH 7.5. The use of a NADPH concentration up to 200 μM is not sufficient to
 6 reduce 200 μM GSSG. Once the NADPH concentration is increased to 400 μM, GorA catalyzes the full conversion.
 7 As shown in figure 5A (see the main paper), the inclusion of GorA within the redox regeneration pathway decreases
 8 the NADP⁺ demand as the reducing equivalents come from an initial electron donor (formate) that is present in the
 9 millimolar range. Data from six replicates (*n* = 6), s.e.m. constitute the error bars.

10

A



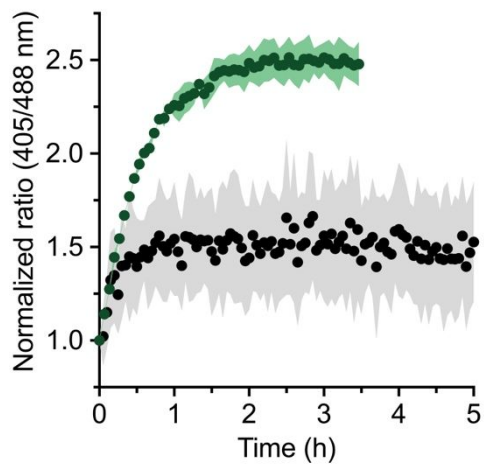
B



1

2 **Fig. S9. Long-term NADPH dynamics in the presence of the glutathione drain in LUVs.** (A) The reduction of both
 3 cofactors NADH and NADPH is followed as increase in fluorescent intensity at the excitation wavelength of 370 nm.
 4 (B) The specific formation of NADPH is reported as a function of the ratiometric readout (420/485) provided by the
 5 encapsulation of the sensor iNap1. The measurements were carried out at 30 °C over a period of 10 hours, upon addition
 6 of 5.0 mM ammonium formate at time = 0.

7



1
 2 **Fig. S10. NADPH formation in GUVs in the presence of a glutathione drain.** Fluorescent readout from giant
 3 vesicles in a microfluidic flow device over time. The reduction of NADP^+ to NADPH upon the addition of external 5.0
 4 mM formate in buffer I, in the presence (black circles, $n=44$) and absence (green circles, $n=114$) of 0.25 μM GorA and
 5 2.5 mM GSSG. The common encapsulated reactants in both the GUVs samples are: 2.0 μM Fdh, 1.0 mM NAD^+ , 0.21
 6 μM SthA, .5 mM NADP^+ , 1.0 μM iNap1, along with the NADPH sensor iNap, from which fluorescent intensities are
 7 measured at 405 and 488 nm excitation.
 8
 9
 10

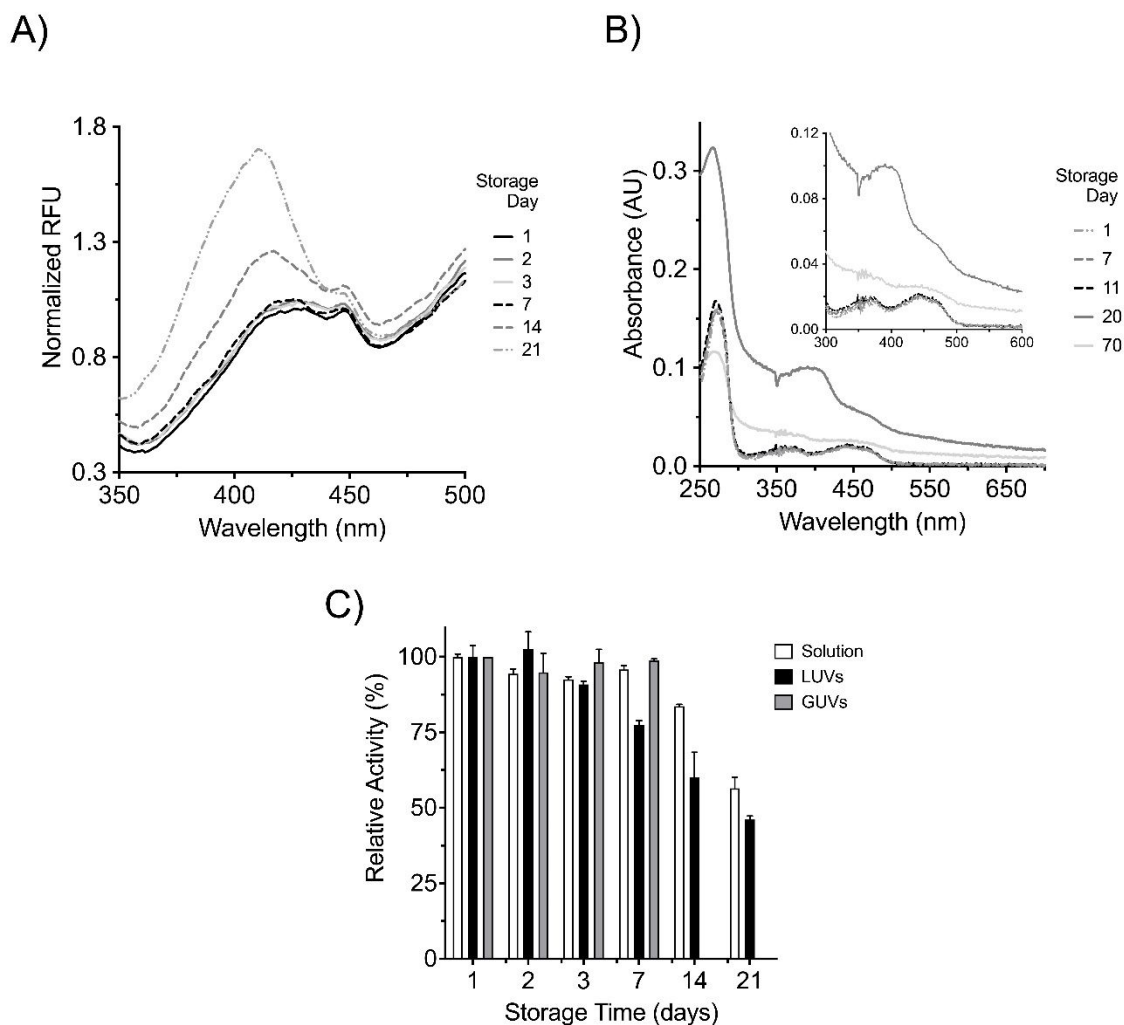
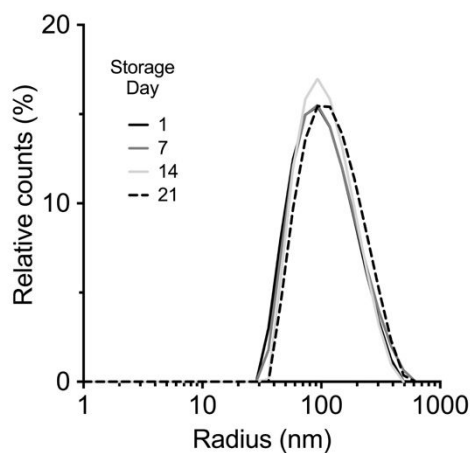


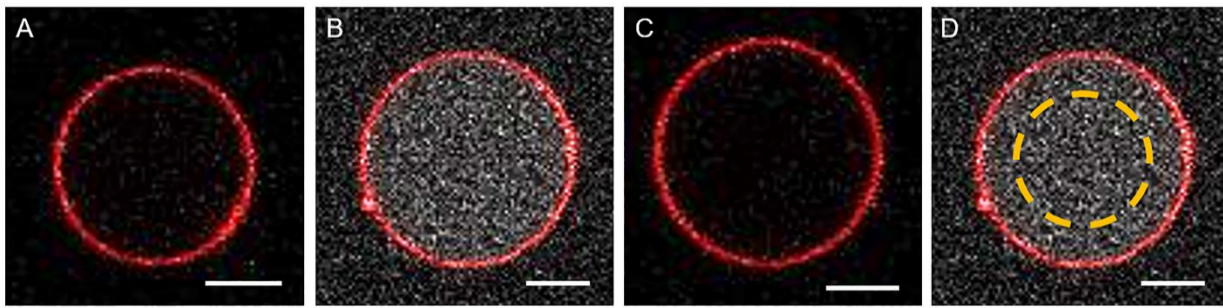
Fig. S11. Stability of the cofactor regeneration pathway inside vesicles. (A) Fluorescence excitation spectrum of the vesicles with the redox pathway. The emission wavelength was 530 nm. The vesicles were encapsulated with the same components used in figure 5C, with 2.5 mM GSSG. (B) The absorbance spectrum of purified SthA (here in bulk solution, not in vesicles) changes during storage at 4 °C. For the transhydrogenase, we observed the appearance of a peak around 400 nm in the absorbance spectrum after 14 days, which reflects the fluorescent peak found over time in the compartmentalized pathway (Supplementary Fig. S10A). Thus, we identified SthA as the critical component for the long-term stability of the redox cofactor regeneration pathway. Similar observations about stability have been reported for soluble transhydrogenases from *E.coli* and *A.vinelandii*. (C) Fdh activity in solution, LUVs and GUVs. The activity was calculated as a percentage of the value on day 1. The formate dehydrogenase from *Starkeya novella* retained high activity over three weeks of storage at 4 °C. In bulk solution, Fdh conserved 95%, 83% and 57% of the original activity after 7, 14 and 21, respectively ($n = 2$). In LUVs, the activity was 91% after 3 days ($n = 2$), which is comparable to 93% for Fdh in solution. For Fdh-containing GUVs, their activity was only measurable up to 1 week after vesicle formation (the vesicles were not stable beyond this point) and the activity at this point was still at 99% ($n = 2$; the average of the analyzed vesicles for individual measurement was 30 ± 5 , for a total of 240 vesicles). In all conditions, the error bars are reported as standard deviation. Such persistence in terms of enzymatic activity even within the lumen of synthetic liposomes confirms this particular bacterial Fdh as a promising tool for a long-lasting regeneration of cofactors.



1

2 **Fig. S12. Structural integrity of large unilamellar vesicles containing Fdh and NAD⁺ over time.** The size
 3 distribution of 400 nm extruded liposomes encapsulating 0.25 μ M Fdh and 0.5 mM NAD⁺ was measured by Dynamic
 4 Light Scattering (DLS) at the constant temperature of 20 °C. The DLS profile was determined for the same sample
 5 immediately after its preparation (day 1, solid black line) and following the storage at 4°C for three weeks (day 7 in
 6 dark grey, 14 in light grey and day 21 in dashed black line), without any further extrusion. The liposomal sample did
 7 not show any significant change in size distribution, excluding on one the hand relevant structural rearrangements of
 8 the compartments, and on the other hand strengthening the conclusion of the loss of activity over time due to enzyme
 9 inactivation.

10



1
2 **Fig. S13. Measuring luminal GUV NADH intensity.** (A) Confocal cross-section of a GUV containing NAD⁺ plus
3 Fdh (1 mM and 4 μM respectively) before the addition of trigger substrate. (B) GUV containing NAD⁺ plus Fdh (1
4 mM and 4 μM respectively) after the addition of sodium formate (5 mM) (C) GUV showing the absence of NADH
5 fluorescence when formic acid (5 mM) has been added to vesicles that do not contain Fdh but do contain NAD⁺ (1
6 mM). (D) Confocal cross section of GUV demonstrating how a region of interest is selected (yellow dashed line) for
7 measuring luminal intensity. GUV membrane is labelled in red, visible via the excitation of 0.1 mol% Atto647N DPPE.
8 NADH excited with 405 nm laser. Scale bar: 5 μm.

9

10

11

1 **Table S1. Primers for cloning.**

Primer	Sequence (5' -> 3')
FdH-Fw FdH-Rv	ATATATGCTCTTCTAGTGCCAAAATTCTGTGCGTGCTGTATG TATATAGCTCTTCATGCACCGGCTTTTTTGAATTTTGCTGCTTC
SthA-Fw SthA-Rv	ATATATGCTCTTCTAGTCCACATTCCTACGATTACGATGCCATAGTAATAGG TATATAGCTCTTCATGCAAACAGGCGGTTTAAACCGTTTAACGCAG
GorA-Fw GorA-Rv	ATATATGCTCTTCTAGTACTAAACACTATGATTACATCGCCATCGGC TATATAGCTCTTCATGCACGCATTGTCACGAACTCTTCTGC
Mdh8hisNcoI-Fw MdhXbaI-Rv	GCGGCCATGGGCCATCATCACCACCATCATCACCATAAAGTCGCAGTCCTCGGCGC GGCCGTCTAGATCATTACTTATTAACGAACTCTTCGCCAGGGC
iNap-Fw iNap-Rv	ATATATGCTCTTCTAGTAACCGGAAGTGGGGCCTGTG TATATAGCTCTTCATGCGCCCATCATCTCCTCCCGCC

2
3

1 **Table S2. Buffers used in this work.**

Name	Composition
A	50 mM KPi pH 7.5, 150 mM NaCl
B	50 mM pH 7.5
C	50 mM KPi pH 7.5, 100 mM NaCl
D	50 mM KPi pH 7.5, 100 mM NaCl, 0.2 μ M Malate dehydrogenase and 0.5 mM oxaloacetic acid
E	2.0 μ M Fdh, 1 mM NAD ⁺ , 50 mM KPi (pH 7.0), 100 mM NaCl.
F	10.0 μ M Fdh, 5 mM NAD ⁺ , 50 mM KPi (pH 7.0), 100 mM NaCl. 2.0 μ M Fdh, 1 mM NAD ⁺ , 0.2 μ M SthA, 0.5 mM NADP ⁺ , 1.0 μ M iNap1, 50 mM KPi (pH 7.0),
G	100 mM NaCl
H	50 mM KPi pH 7.0
I	50 mM KPi pH 7.0, 5 mM sodium formate
J	50 mM KPi pH 7.0, 0.5 mM sodium formate

2
3

1 Plasmid maps

2
3 pMA-RQ SNoFdH (3547 bp) provided by Invitrogen ThermoFisher Scientific

4
5 CTAAATTGTAAGCGTTAATATTTTGTAAAATTCGCGTTAAATTTTTGTAAATCAGCTCATTITTTAACC
6 AATAGGCCGAAATCGGCAAATCCCTTATAAATCAAAGAATAGACCGAGATAGGGTTGAGTGGCCG
7 CTACAGGGCGCTCCCATTCGCCATTAGGCTGCGCAACTGTTGGGAAGGGCGTTTCGGTGCGGGCC
8 TCTTCGCTATTACGCCAGCTGGCGAAAGGGGGATGTGCTGCAAGGCGATTAAGTTGGGTAACGCCAG
9 GGTTTTCCAGTCACGACGTTGTAAAACGACGGCCAGTGAGCGCGACGTAATACGACTCACTATAGG
10 GCGAATTGGCGGAAGGCCGTCAAGGCCGCAT **ATGGCCAAAATTCTGTGCGTGCTGATGATGATCC**
11 **GGTTGATGGTTATCCGAAAACCTATGCACGTGATGATCTGCCGAAAATCGATCATTATCCTGGTGGT**
12 **CAGACCTGCCGACCCGAAAGCAATTGATTTTACACCGGGTGCACCTGCTGGGTAGCGTTAGCGGT**
13 **GAACCTGGTCTGCGTAAATATCTGGAAGCAAATGGTCATACCTTTGTTGTGACCAGCGATAAAGAT**
14 **GGTCCGGATAGCGTTTTTGAACGTGAACGTGGTTGATGCCGATGTTGTTATTAGCCAGCCGTTTTGGC**
15 **CTGCATATCTGACACCGGAACGTATTGCAAAGGCCAAAATCTGAAACTGGCACTGACCGCAGGTA**
16 **TTGGTAGCGATCATGTTGATCTGCAGAGCGCAATTGATCGTGGTATTACCGTTGCAGAAGTTACCTA**
17 **TTGTAATAGCATTAGCGTTGCCGAACATGTGGTGATGATGATTCTGGGTTTAGTGCGTAACTATATT**
18 **CCGAGCCATGATTGGGCACGTAAAGGTGGTTGGAATATTGCAGATTGTGTGGAACATTCCTATGAT**
19 **CTGGAAGGCATGACCGTTGGTAGCGTTGCAGCAGGTCGTATTGGTCTGGCAGTTCTGCGTCGCTG**
20 **GCACCGTTTGTGTTAACTGCATTATACCGATCGTCATCGTCTGCCGGAAGCAGTTGAAAAAGAAT**
21 **TAGGTCTGGTTTGGCATGATACCCGTGAAGATATGTATCCGCATTGTGATGTGGTTACCCTGAATGT**
22 **TCCGCTGCATCCGGAACCGAACATATGATTAATGATGAAACCCTGAAGCTGTTTAAACGCGGTGC**
23 **CTATATTGTTAATACCGCACGTGGTAACTGGCAGATCGTGATGCAATTGTTGTCGCAATTGAAAGC**
24 **GGTCAGCTGGCAGGTTATGCCGGTGTGTGGTTTCCGCAGCCTGCACCGAAAGATCATCCGTGG**
25 **CGTACCATGAAATGGGAGGGTATGACACCGCATATTAGCGGCACCAGCCTGAGCGCACAGGCACG**
26 **TTATGCGGCAGGCACCCGTGAAATTCTGGAATGTTTTTTGAAGGTCGTCCGATTTCGTGATGAATAT**
27 **CTGATTGTTCAAGGTGGTGCACCTGGCAGGTACAGGTGCACATAGCTATAGCAAAGGTAATGCAACC**
28 **GGTGGTAGCGAAGAAGCAGCAAAATTCAAAAAGCCGGTTAACTGGGCCTCATGGGCCTTCCGCT**
29 **CACTGCCCGCTTTCCAGTCGGGAAACCTGTCTGTCAGCTGCATTAACATGGTCATAGCTGTTTCCTT**
30 **GCGTATTGGGCGCTCTCCGCTTCTCGCTCACTGACTCGCTGCGCTCGGTCGTTCCGGTAAAGCCTG**
31 **GGTGCCTAA **TGAGCAAAGGCCAGCAAAAGGCCAGGAACCGTAAAAAGGCCGCGTTGCTGGCGT****
32 **TTTTCCATAGGCTCCGCCCCCTGACGAGCATCACAAAATCGACGCTCAAGTCAGAGGTGGCGAA**
33 **ACCCGACAGGACTATAAAGATACCAGGCGTTTCCCCCTGGAAGCTCCCTCGTGCCTCTCCTGTTT**
34 **CGACCCTGCCGTTACCGGATACCTGTCCGCCTTCTCCCTTCGGGAAGCGTGGCGCTTCTCATA**
35 **GCTCACGCTGTAGGTATCTCAGTTCGGTGTAGGTGTTGCTCCAAGCTGGGCTGTGTGCACGAAC**
36 **CCCCGTTCCAGCCGACCGCTGCGCCTTACCGGTAACCTATCGTCTTGAGTCCAACCCGGTAAGAC**
37 **ACGACTTACGCCACTGGCAGCAGCCACTGTTAACAGGATTAGCAGAGCGAGGTATGTAGGCGGT**
38 **GCTACAGAGTTCCTGAAGTGGTGGCCTAACTACGGCTACACTAGAAGAACAGTATTTGGTATCTGC**
39 **GCTCTGCTGAAGCCAGTTACCTTCGGAAAAGAGTTGGTAGCTCTTGATCCGGCAAACAAACCACC**
40 **GCTGGTAGCGGTGGTTTTTTTTGTTTGAAGCAGCAGATTACGCGCAGAAAAAAGGATCTCAAGAA**
41 **GATCCTTTGATCTTTTCTACGGGGTCTGACGCTCAGTGGAACGAAAACCTCACGTTAAGGGATTTTGGT**
42 **CATGAGATTATCAAAAAGGATCTTACCTAGATCCTTTTAAATTAATAAATGAAGTTTTAAATCAATCTAA**
43 **AGTATATATGAGTAACTTGGTCTGACAGTTACCAATGCTTAATCAGTGAGGCACCTATCTCAGCGAT**
44 **CTGTCTATTTTCGTTTCCATAGTTGCCTGACTCCCCGTCGTGTAGATAACTACGATACGGGAGGGC**
45 **TTACCATCTGGCCCCAGTGCTGCAATGATACCGCGAGAACCACGCTCACCGGCTCCAGATTTATCA**
46 **GCAATAAACCAGCCAGCCGGAAGGGCCGAGCGCAGAAGTGGTCTGCAACTTTATCCGCCTCCAT**
47 **CCAGTCTATTAATTGTTGCCGGGAAGCTAGAGTAAGTAGTTCGCCAGTTAATAGTTTGCACAACGTT**
48 **GTTGCCATTGCTACAGGCATCGTGGTGTACGCTCGTCTTTGGTATGGCTTCATTCAGCTCCGTT**
49 **CCCAACGATCAAGGCGAGTTACATGATCCCCATGTTGTGCAAAAAGCGGTTAGCTCCTTCGGTC**
50 **CTCCGATCGTTGTGAGAAGTAAGTTGGCCGCACTGTTATCACTCATGGTTATGGCAGCACTGCATAA**
51 **TTCTCTTACTGTCATGCCATCCGTAAGATGCTTTTCTGTGACTGGTGAGTACTCAACCAAGTCATTCT**
52 **GAGAATAGTGATGCGGCGACCGAGTTGCTCTTGCCCGGCGTCAATACGGGATAATACCGCGCCA**
53 **CATAGCAGAACTTTAAAAGTGCTCATCATTGGAAAACGTTCTTCCGGGGCGAAAACCTCAAGGATC**
54 **TTACCGCTGTTGAGATCCAGTTCGATGTAACCCACTCGTGCACCCAACCTGATCTTCAGCATCTTTTA**
55 **CTTTCACCAGCGTTTCTGGGTGAGCAAAAACAGGAAGGCAAAATGCCGCAAAAAGGGAATAAGG**
56 **GCGACACGGAAATGTTGAATACTCATACTCTTCTTTTCAATATTATTGAAGCATTATCAGGGTTAT**
57 **TGTCTCATGAGCGGATACATATTTGAATGTATTTAGAAAAATAACAAATAGGGGTTCCGCGCACATTT**
58 **CCCCGAAAAGTGCCAC**

59 - Ampicillin Resistance

- 1 - Col E1 Origin
- 2 - Codon-optimized formate dehydrogenase gene from *Starkeya novella* for
- 3 expression in *E.coli*
- 4

GACGGATCGGGAGATCTCCCGATCCCCTATGGTGCCTCTCAGTACAATCTGCTCTGATGCCGCATA
GTTAAGCCAGTATCTGCTCCCTGCTTGTGTGTTGGAGGTCGCTGAGTAGTGCGCAGCAAATTTAA
GCTACAACAAGGCAAGGCTTGACCGACAATTGCATGAAGAATCTGCTTAGGGTTAGGCGTTTTGCGC
TGCTTCGCGATGTACGGGCCAGATATACGCGTTGACATTGATTATTGACTAGTTATTAATAGTAATCAA
TTACGGGGTCATTAGTTCATAGCCCATATATGGAGTTCGCGTTACATAACTTACGGTAAATGGCCCG
CCTGGCTGACCGCCCAACGACCCCGCCATTGACGTCAATAATGACGTATGTTCCCATAGTAACGC
CAATAGGGACTTTCATTGACGTCAATGGGTGGAGTATTTACGGTAAACTGCCCACTTGGCAGTACAT
CAAGTGTATCATATGCCAAGTACGCCCCCTATTGACGTCAATGACGGTAAATGGCCCGCCTGGCATT
TGCCCAGTACATGACCTTATGGGACTTTCCTACTTGGCAGTACATCTACGTATTAGTCATCGCTATTAC
CATGGTGATGCGGTTTTGGCAGTACATCAATGGGCGTGGATAGCGGTTTGACTCACGGGGATTTCCA
AGTCTCCACCCATTGACGTCAATGGGAGTTTGTGGCCACAAAATCAACGGGACTTTCAAAATG
TCGTAACAACCTCCGCCCATGACGCAAATGGGCGGTAGGCGGTACGGTGGGAGGTCTATATAAGC
AGAGCTCTCTGGCTAACTAGAGAACCCTACTGCTTACTGGCTTATCGAAATTAATACGACTCACTATAG
GGAGACCCAAAGCTGGCTAGCGCCACCATGGATCCGATGAACCGGAAGTGGGGCCTGTGCATCGTG
GGCATGGGCGGGTGGCAGCGCCCTGGCCGACTACCCCGCTTCGGCGAGAGCTTCGAGCTGC
GGGGCTTTCAGCCGCGAGCCCAAGAAGGTGGCCGCGCCGCTGCGGGGCGGGCTGATCGAGCA
CGTAGATCTGCTGCCCCAGCGGGTGCCCGCCGGATCGAGATCGCCCTGCTGACCGTGCCCCGGG
AGGCCGCCAGAAGGCCGCGACCTGCTGGTGGCCGCGGCATCAAGGGCATCCTGAACCTCGCA
CCGGTGGTGCTGGAGGTGCCAAGGAGGTGGCCGTGGAGAACGTGGACTTCTCTGCAGGCTACAA
CAGCGACAACGTCTATATCATGGCCGACAAGCAGAAGAACGGCATCAAGGCCAACTTCAAGATCC
GCCACAACGTGAGGACGGCAGCGTGCAGCTCGCCGACCACTACCAGCAGAACACCCCATCGG
CGACGGCCCCGTGCTGCTGCCGACAACCACTACCTGAGCTTCCAGTCCGTCCTGAGCAAAGACC
CCAACGAGAAGCGCGATCACATGGTCTGCTGGAGTTCGTGACCGCCGCGGGATCACTCTCGGC
ATGGACGAGCTGTACAACGTGGATGGCGGTAGCGGTGGCACCGGCAGCAAGGGCGAGGAGCTGT
TCACCGGGTGGTGGCCATCCTGGTGCAGCTGGACGGCGACGTAACGGCCACAAGTTCAGCGTG
TCCGGCGAGGGCGAGGGCGATGCCACCTACGGCAAGCTGACCCTGAAGCTGATCTGCACCACCG
GCAAGCTGCCCGTGCCCTGGCCACCCCTCGTGACCACCCCTCGGCTACGGCCTGAAGTGCTTCGCC
CGCTACCCCGACCACATGAAGCAGCAGACTTCTTCAAGTCCGCCATGCCCGAAGGCTACGTCCA
GGAGCGCACCATCTTCTTCAAGGACGACGGCAACTACAAGACCCGCGCCGAGGTGAAGTTCGAGG
GCGACACCCTGGTGAACCGCATCGAGCTGAAGGGCATCGGCTTCAAGGAGGACGGCAACATCCTG
GGGACAAGCTGGAGTACAACGGTCTGGCCGGCCTGACCCGGCTGAGCTTCGCCATCCTGAACCC
CAAGTGGCGGGAGGAGATGATGGGCAAGCTTCTAGAGGGCCCGTTAAACCCGCTGATCAGCCTC
GACTGTGCCTTCTAGTTGCCAGCCATCTGTTGTTTGGCCCTCCCCCGTGCCTTCTTGACCCTGGAAG
GTGCCACTCCCACTGTCCTTTCCTAATAAAATGAGGAAATTGCATCGCATTGTCTGAGTAGGTGTCATT
CTATTCTGGGGGTGGGGTGGGGCAGGACAGCAAGGGGGAGGATTGGGAAGACAATAGCAGGCAT
GCTGGGGATGCGGTGGGTCTATGGCTTCTGAGGCGGAAAGAACCAGCTGGGGCTCTAGGGGGTAT
CCCCACGCGCCCTGTAGCGGCGCATTAAAGCGCGCGGGTGTGGTGGTTACGCGCAGCGTGACCGC
TACACTTGCCAGCGCCCTAGCGCCCGCTCCTTTCGTTTTCTTCCCTTCTTCTCGCCACGTTTCGCCG
GCTTTCGCCGTAAAGCTCTAAATCGGGGGCTCCCTTAGGGTTCCGATTTAGTGTATTACGGCACCCTC
GACCCCAAAAAACTTGATTAGGGTATGGTTCAGTGTAGTGGCCATCGCCCTGATAGACGGTTTTTC
GCCCTTGGAGTTGGAGTCCACGTTCTTTAATAGTGCATCTTGTTCCAAACCTGGAACAACACTCAAC
CCTATCTCGGTCTATTCTTTGATTTATAAGGGATTTGCCGATTCGGCCTATTGGTTAAAAAATGAG
CTGATTTAACAAAAATTAACGCGAATTAATTCTGTGGAATGTGTGTCAGTTAGGGTGTGGAAAGTCCC
CAGGCTCCCAGCAGGCAGAAGTATGCAAAGCATGCATCTCAATTAGTCAGCAACCAGGTGTGGAAA
GTCCCAGGCTCCCAGCAGGCAGAAGTATGCAAAGCATGCATCTCAATTAGTCAGCAACCATAGTC
CCGCCCTAACTCCGCCCATCCCGCCCTAACTCCGCCAGTTCCGCCATTCTCCGCCCATGGCT
GACTAATTTTTTTTTATTTATGCAGAGGCCGAGGCCGCTCTGCCTCTGAGCTATTCCAGAAGTAGTGA
GGAGGCTTTTTTGGAGGCCTAGGCTTTTGCAAAAAGCTCCCGGGAGCTTGTATATCCATTTTCGGATC
TGATCAGCACGTGATGAAAAAGCCTGAACTCACCGCGACGTCTGTGAGAAGTTTCTGATCGAAAAGT
TCGACAGCGTCTCCGACCTGATGCAGCTCTCGGAGGGCGAAGAATCTCGTGCTTTCAGCTTCGATGT
AGGAGGGCGTGGATATGTCTGCGGGTAAATAGCTGCGCCGATGGTTTCTACAAAGATCGTTATGTT
TATCGGCACTTTGCATCGGCCGCGCTCCCGATTCCGGAAGTGCTTGACATTGGGAATTCAGCGAGA
GCCTGACCTATTGCATCTCCCGCCGTGCACAGGGTGTACGTTGCAAGACCTGCCTGAAACCGAACT
GCCCGCTGTTCTGCAGCCGGTCGCGGAGGCCATGGATGCGATCGCTGCGGCCGATCTTAGCCAGAC
GAGCGGGTTCGGCCATTCCGACCGCAAGGAATCGGTCAATACACTACATGGCGTGATTTATATGC
GCGATTGCTGATCCCCATGTGTATCACTGGCAAACGTGATGGACGACACCGTCAGTGCGTCCGTCG
CGCAGGCTCTCGATGAGCTGATGCTTTGGGCCGAGGACTGCCCGAAGTCCGGCACCTCGTGACCG
CGGATTTCCGGCTCCAACAATGTCTGACGGACAATGGCCGCATAACAGCGGTCAATTGACTGGAGCGA

1 GCGATGTTCCGGGATTCCCAATACGAGGTCGCCAACATCTTCTTCTGGAGGCCGTGGTTGGCTTGT
2 ATGGAGCAGCAGACGCGCTACTTCGAGCGGAGGCATCCGGAGCTTGCAGGATCGCCGCGGCTCCG
3 GCGTATATGCTCCGCATTGGTCTTGACCAACTCTATCAGAGCTTGGTTGACGGCAATTTTCGATGATG
4 CAGCTTGGGCGCAGGGTCGATGCGACGCAATCGTCCGATCCGGAGCCGGGACTGTCCGGCGTACA
5 CAAATCGCCCCGAGAAGCGCGGCCGTCTGGACCGATGGCTGTGTAGAAGTACTCGCCGATAGTGA
6 AACCGACGCCCCAGCACTCGTCCGAGGGCAAAGGAATAGCACGTGCTACGAGATTTTCGATTCCACCG
7 CCGCCTTCTATGAAAGGTTGGGCTTCGGAATCGTTTTCCGGGACGCCGGCTGGATGATCCTCCAGCG
8 CGGGGATCTCATGCTGGAGTTCTTCGCCACCCCAACTTGTATTGCAGCTTATAATGGTTACAAAT
9 AAAGCAATAGCATCACAATTTCAAAATAAAGCATTTTTTCACTGCATTCTAGTTGTGGTTTTGCCAA
10 ACTCATCAATGTATCTTATCATGTCTGTATACCGTCGACCTCTAGCTAGAGCTTGGCGTAATCATGGTC
11 ATAGCTGTTTCTGTGTGAAATTGTTATCCGCTCACAATTCACACAACATACGAGCCGGAAGCATAA
12 AGTGTAAGCCTGGGGTGCCTAATGAGTGAGCTAACTCACATTAATTGCGTTGCGCTCACTGCCCGC
13 TTTCCAGTCGGGAAACCTGTCTGTCGAGCTGCATTAATGAATCGGCCAACGCGCGGGGAGAGGGCG
14 TTTGCGTATTGGGCGCTCTCCGCTTCCTCGCTCACTGACTCGCTGCGCTCGGTCGTTCCGGCTGCGG
15 CGAGCGGTATCAGCTCAAAAGGCGGTAATACGGTTATCCACAGAATCAGGGGATAACGCAGGAA
16 AGAACATGTGAGCAAAAGGCCAGCAAAAGGCCAGGAACCGTAAAAAGGCCGCGTTGCTGGCGTTTTT
17 CCATAGGCTCCGCCCCCTGACGAGCATCACAATAATCGACGCTCAAGTCAGAGGTGGCGAAACCC
18 GACAGGACTATAAAGATACCGGCTTTCCCGCTGGAAGCTCCCTCGTGCGCTCTCCTGTTCCGACC
19 CTGCCGCTTACCGGATACCTGTCCGCTTTCTCCCTTCGGGAAGCGTGCGCTTTCTCATAGCTCAC
20 GCTGTAGGTATCTCAGTTTCGGTGTAGGTCGTTCCGCTCCAAGCTGGGCTGTGTGCACGAACCCCGT
21 TCAGCCCGACCGCTGCGCCTTATCCGGTAACTATCGTCTTGTGAGTCCAACCCGGTAAGACACGACTTA
22 TCGCCACTGGCAGCAGCCACTGGTAACAGGATTAGCAGAGCGAGGTATGTAGGCGGTGCTACAGAG
23 TTCTTGAAGTGGTGGCCTAACTACGGCTACACTAGAAGAACAGTATTTGGTATCTGCGCTCTGCTGAA
24 GCCAGTTACCTTCGGAAAAAGAGTTGGTAGCTCTTGATCCGGCAAACAAACCACCGCTGGTAGCGGT
25 TTTTTGTTTGAAGCAGCAGATTACGCGCAGAAAAAAGGATCTCAAGAAGATCCTTTGATCTTTTCT
26 ACGGGGTCTGACGCTCAGTGGAACGAAAACCTCACGTTAAGGGATTTTGGTTCATGAGATTATCAAAAAG
27 GATCTTCACCTAGATCCTTTTAAATTAATAAATGAAGTTTTAAATCAATCTAAAGTATATATGAGTAACTT
28 GGTCTGACAGTTACCAATGCTTAATCAGTGAGGCACCTATCTCAGCGATCTGTCTATTTTCGTTTCATC
29 CATAGTTGCCTGACTCCCGTCGTGTAGATAACTACGATACGGGAGGGCTTACCATCTGGCCCCAG
30 TGCTGCAATGATACCGCGAGACCCACGCTCACCGGCTCCAGATTTATCAGCAATAAACCAGCCAGC
31 CGGAAGGGCCGAGCGCAGAAGTGGTCTGCAACTTTATCCGCTCCATCCAGTCTATTAATTGTTG
32 CCGGAAGCTAGAGTAAGTAGTTCGCCAGTTAATAGTTTTCGCAACGTTGTTGCCATTGCTACAGG
33 CATCGTGGTGTACGCTCGTCGTTTGGTATGGCTTCATTCAGCTCCGGTTCCTCAACGATCAAGGCG
34 AGTTACATGATCCCCATGTTGTGCAAAAAAGCGGTTAGCTCCTTCGGTCTCCGATCGTTGTCAGA
35 AGTAAGTTGGCCGAGTGTATCACTCATGGTTATGGCAGCACTGCATAATTCTTACTGTTCATGC
36 CATCCGTAAGATGCTTTTCTGTGACTGGTGTGACTCAACCAAGTCATTCTGAGAATAGTGTATGCG
37 GCGACCGAGTTGCTCTTGGCCGGCGTCAATACGGGATAATACCGCGCCACATAGCAGAACTTTAAA
38 AGTGCTCATCATTGGAAAACGTTCTTCGGGGCGAAAACCTCTCAAGGATCTTACCGCTGTTGAGATC
39 CAGTTCGATGTAACCCACTCGTGCACCCAACTGATCTTCAGCATCTTTACTTTTACCAGCGTTTCTG
40 GGTGAGCAAAAACAGGAAGGCAAATGCCGCAAAAAAGGGAATAAGGGCGACACGGAAATGTTG
41 AATACTCATACTCTTCTTTTCAATATTATTGAAGCATTTATCAGGGTTATTGTCTCATGAGCGGATAC
42 ATATTTGAATGTATTTAGAAAAATAAACAATAGGGGTTCCGCGCACATTTCCCCGAAAAGTGCCACCT
43 GACGTC

- 44
- 45 - **iNAP1 sequence**
- 46 - **Ampicillin Resistance**
- 47

48
49